2_C23

# Numerical Evaluations of a Multiple 3D Particle Tracking Velocimetry System for Indoor Air Flow Study

**M. Nedaei** **K. Kant, PhD** **P. H. Biwole, PhD**

**E. Deckneuvel, PhD** **Gilles Jacquemod, PhD** **F. Pennec, PhD**

**F. Labesse-Jied, PhD**

**ABSTRACT**

*High-quality data obtained from three-dimensional Particle Tracking Velocimetry (3D PTV) is pivotal for indoor environment engineering when designing ventilation strategies or monitoring airborne pollutants dispersion in inhabited spaces. A new method is proposed to link multiple 3D PTV systems, positioned side by side so that the entire measuring volume can be covered. An algorithm is developed to establish a link between the particles' trajectories calculated by each 3D PTV system. To evaluate the validity and robustness of the multi-PTV algorithm, synthetic particles were created, which follow different motions implemented in Matlab, including two analytical solutions for incompressible Navier-Stokes equations, namely Kovasznay and Beltrami flows, as well as a linear motion. Two different tracking algorithms were used to obtain 3D particle positions. The numerical results reveal that the proposed method is capable of connecting adjacent multiple PTV systems with reasonable accuracy and therefore can be considered as a promising method for indoor airflow measurements.*

**M. Nedaei** was PhD student at Université Clermont Auvergne, CNRS, Clermont Auvergne INP, Institut Pascal, F-63000 Clermont–Ferrand, France. **K. Kant** is post-doctoral researcher at Université Clermont Auvergne, CNRS, Clermont Auvergne INP, Institut Pascal, F-63000 Clermont–Ferrand, France. **P. H. Biwole, F. Labesse-Jied** and **F. Pennec** are professors at Université Clermont Auvergne, CNRS, Clermont Auvergne INP, Institut Pascal, F-63000 Clermont–Ferrand, France. **E. Deckneuvel and G. Jacquemod** are professors at Université Côte d'Azur, Polytech'Lab, EA UNS 7498, Sophia Antipolis, France.

## INTRODUCTION

Three-dimensional particle tracking velocimetry (3D PTV) is the quantitative measurement of flow velocity and trajectory through 3D tracking of neutrally buoyant discrete particles immersed in a fluid. The observation of the fluid is performed using at least three time-synchronous cameras viewing the fluid from widely separated directions. Each particle is individually tracked thus providing a non-intrusive and Lagrangian understanding of the flow. More details on the basic principles of 3D PTV can be found in a large number of scientific papers such as (Adrian 1991). Though applicable for a wide variety of applications such as the optimization of oxygen dispersion in bio-fuel reactors, the understanding of swarm behavior, or even car traffic modeling, 3D PTV has mainly been developed and used for fluid flow characterization and computational fluid dynamics validation. 3D PTV is now increasingly searched for large-scale (above 1 cubic meter) indoor airflow study, with current systems covering volumes up to 4.2m (L) × 3.0m (W) × 3.6m (H) (Resagk et al. 2006). In buildings, large-scale 3D PTV is a promising asset in the field of indoor air engineering, to study isothermal and non-isothermal turbulent convection structures in rooms (Biwole 2009), to monitor the dispersion of airborne contaminants (Wei 2010) and to design new ventilation strategies (O'Sullivan et al. 2014). 3D PTV can complete or overcome the limitations of most traditional measurement methods which are intrusive such as hot wire (Popiolek et al. 1998). This study aims to resolve the current limitation of the measuring volume by positioning several PTV systems side by side. This limitation prevents applying 3D PTV with a suitable spatial resolution for the characterization of the airflow in large enclosures such as auditoriums.

## METHODS

### Multi PTV systems camera calibration

Multi-camera calibration is a procedure to define a common 3D reference frame for particle coordinates. Firstly, each PTV system should be calibrated separately to determine intrinsic and extrinsic parameters. The calibration parameters are generally calculated based on the minimization of the reprojection error between the known 3D coordinates of the calibration target and the same coordinates calculated via a mathematical camera model. Here, the calibration method proposed by Zhang (1999) and the pinhole camera mathematical model suggested by Heikkila and Silven (1997) were employed. For the sake of clarity, we assume that there are only two 3D PTV systems, system ($m$) and system ($n$), each system is composed of three cameras. Secondly, a common 3D reference frame for all 3D PTV systems should be defined. One indispensable requirement is that at least one camera should have a view over the calibration target of the other system. Within system ($n$), the relationship between camera $i$ 3D reference frame $XX_{Ci}^{(n)}$ and system (n) 3D reference frame $XX^n$ reads:

$$XX_{Ci}{}^{(n)} = R_i{}^{(n)}.XX^{(n)} + T_i{}^{(n)} \tag{1}$$

where $R_i^{(n)}$ and $T_i^{(n)}$ are the extrinsic parameters of camera $i$ in the system ($n$). If camera $i$ of the system ($n$) sees the calibration target position defining the 3D reference frame of the system ($m$) noted $XX^{(m)}$, then:

$$XX_{ci}{}^{(n)} = R_i{}^{(m)}.XX^{(m)} + T_i{}^{(m)} \tag{2}$$

where $R_i^{(m)}$ and $T_i^{(m)}$ are the extrinsic parameters of camera $i$ in the system ($m$). From equations (1) and (2), the relationship between 3D coordinates systems $XX^{(m)}$ and $XX^{(n)}$ reads:

$$XX^{(n)} = \left[R_i{}^{(n)}\right]^{-1}\left[R_i{}^{(m)}.\ XX^{(m)} + T_i{}^{(m)} - T_i{}^{(n)}\right] \tag{3}$$

Taking as an example the two 3D PTV systems shown in Fig. 1 and assuming that camera 6 of system (2) has a view on the calibration target of system 1, the previous reasoning leads to:

$$XX^{(2)} = \left[R_6{}^{(2)}\right]^{-1}\left[R_6{}^{(1)}.\ XX^{(1)} + T_6{}^{(1)} - T_6{}^{(2)}\right] \tag{4}$$

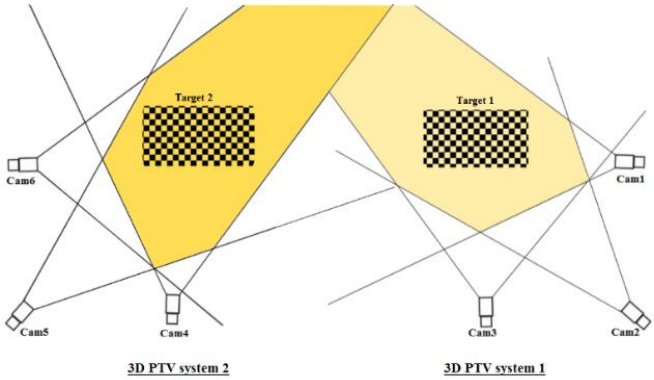


Fig. 1. Camera 6 of the system (2) has a view on the calibration target of the system (1).

## Tracking algorithms

Two different tracking algorithms were used to determine the synthetic particle trajectories and velocities as shown in Fig. 2. To calculate particle centers, the weight-averaged method is applied due to its simple implementation and efficient computation. In Alg. I proposed by Biwole (2009), spatial matching is done first, based on the particles' 3D coordinates calculated by triangulation from three cameras simultaneously using all particle center pixel coordinates. Then temporal tracking is conducted using a modified fast-normalized cross-correlation (Eq. 5) in the 2D image plane.

$$\gamma(u,v) = \frac{\Sigma_{x,y}[f(x,y)-\bar{f}_{u,v}][t(x-u,y-v)-\bar{t}]}{\sqrt{\Sigma_{x,y}[f(x,y)-\bar{f}_{u,v}]^2 \Sigma_{x,y}[(t(x-u,y-v)-\bar{t}]^2}} \tag{5}$$

where $f$ is the research window, $\bar{t}$ is the mean of the template, and $\bar{f}_{u,v}$ is the mean of $f(x,y)$ in the template region. When there is more than one correlation peak, a procedure using the Lagrangian extrapolation of an estimate position using the last two or three positions of the particle is applied. 3D reconstruction is conducted using the least-squares method. Alg. II suggested by Barker (2012) makes use of epipolar constraint by using the fundamental matrix of each pair of cameras for spatial matching and tracking is performed in 3D space. 'Priority strict' scheme is used to initialize the particle trajectories between the first two frames and estimates the particle's position in the new frame using an approximation of velocity through the first-order backward difference scheme, as given by Eq. (6) and (7).

$$x_{pre}^{t+1} = x^t + u^t \Delta T \tag{6}$$

$$u^t = \frac{x^t - x^{t-1}}{\Delta T} + O(\Delta T) \tag{7}$$

where $x_{pre}^{t+1}$ is the estimated particle's position and $u^t$ its velocity at frame $t$. A search radius based on the magnitude of velocity multiplied by the time is calculated. Finally, a cost function is applied to find the matched tracked particle position.

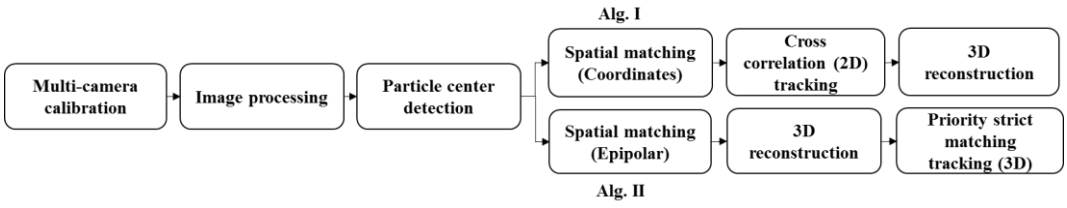


Fig. 2. Flow chart of the two different tracking algorithms applied.

### Synthetic particles

Synthetic images were generated using in-house codes written in MATLAB. 3D coordinates of 500 particles were randomly generated for one PTV system. Particles are disk-shaped white patterns in 3×3 matrices with varying luminance. All particles are given three types of displacements, including linear, 3D laminar macro scale flows of known Navier–Stokes solutions, namely the 2D Kovasznay and 3D Beltrami flow, as given in Eq. (8) and (9) respectively (Ethier and Steinman 1994). The Reynolds number, *Re* is set to 40.

$$\begin{cases} v_x = 1 - exp(\lambda x)\, cos(2\pi y)\,, v_y = \frac{\lambda}{2\pi}\, exp(\lambda x)\ sin(2\pi y) \\ \lambda = Re/2 - (Re^2/4 + 4\pi^2)^{0.5} \end{cases} \tag{8}$$

$$\begin{cases} v_x = -a(e^{ax}\sin(ay+dz) + e^{az}\cos(ax+dy))e^{-d^2vt} \\ v_y = -a(e^{ay}\sin(az+dx) + e^{ax}\cos(ay+dz))e^{-d^2vt} \\ v_z = -a(e^{az}\sin(ax+dy) + e^{ay}\cos(az+dx))e^{-d^2vt} \end{cases} \tag{9}$$

where $v_x$, $v_y$ and $v_z$ are velocity vector components, $a = \pi/4$, $d = \pi/2$, $v$ = 0.025 and $t$ = 0. The displacement of particles in 3D space should be such that they cross the adjacent PTV system throughout a chosen number of frames ($n_f = 120$). The 3D coordinates generated for system (1) are transformed into the 3D coordinates of calibration target (2) reference frame using Eq. (4). Lastly, each frame is back-projected on the 2D image space of each camera according to its calibration parameters.

### Linking trajectories from separate 3D PTV systems

This section introduces a method to establish a link among the particle trajectories separately calculated for each 3D PTV system. There should be a non-zero intersection in the 3D fields observed by the two adjacent systems. Two 3D coordinates of the two 3D PTV systems are considered to be "similar", meaning that they correspond to the same particle, if the Euclidean distance between them, noted below as A and B, is lower or equal than a threshold value s:

$$\|A - B\|_2 = \sqrt{(x_A - x_B)^2 + (y_A - y_B)^2 + (z_A - z_B)^2} \leq s \tag{10}$$

If this similarity criterion is valid for at least three consecutive instants, then the algorithm proceeds to link the trajectories related to those particles, $XX^{(1)}$ and $XX^{(2)}$.

## RESULTS AND DISCUSSION

The evaluations are based on the 'matching ratio' index which is defined as the number of 3D tracked positions correctly matched between the two PTV systems divided by the total number of 3D positions, versus the tracking density index, which is the ratio of the mean particle spacing in the nearest neighbor sense to the mean displacement of particles between two consecutive frames. The tracking density index reflects the tracking difficulty, the bigger its value, the easier the tracking. The number of frames was set to 50 to 90 in order to cover the intersection area between the two systems. Whatever the 3D PTV algorithm, the number of tracked frames should be limited, in order to obtain accurate results. Fig. 3a, b and c shows matching ratio with respect to tracking density for two 3D PTV algorithms on the condition of predefined linear flow, Kovasznay flow, with no particle motion in the z-direction and 3D Beltrami flow, respectively. As can be seen, algorithm II always yields better results than algorithm I, where the matching ratio increases with an increase in tracking density. When the epipolar constraint is adopted for spatial matching, a higher matching ratio can be obtained. The numerical results obtained reveal that tracking density has a strong influence on the performance of the algorithms. As can be seen in the graphs, in the ideal case, where the tracking is not performed and synthetic particles 3D positions were directly used as the input to match the particles between the two systems, all the particles are perfectly matched. It can be therefore concluded that the accuracy of our proposed method for connecting multiple 3D PTV systems to cover larger areas is highly dependent on the performance of the measurement algorithms, as the core part of the PTV system. Hence, applying an algorithm with high accuracy can result in a higher number of particles paired between the two 3D PTV systems. Alg. I is used to showing the effect of threshold *s* varying from 1 to 9, on the number of frames matched between the two PTV systems (Fig. 4). The average tracking density is taken into account. As the threshold increases, the number of frames associated with the same particles increases, which means that the system is capable of tracking longer trajectories in the intersection area. However, increasing the threshold may lead to false particle matching in the case of low tracking density index.

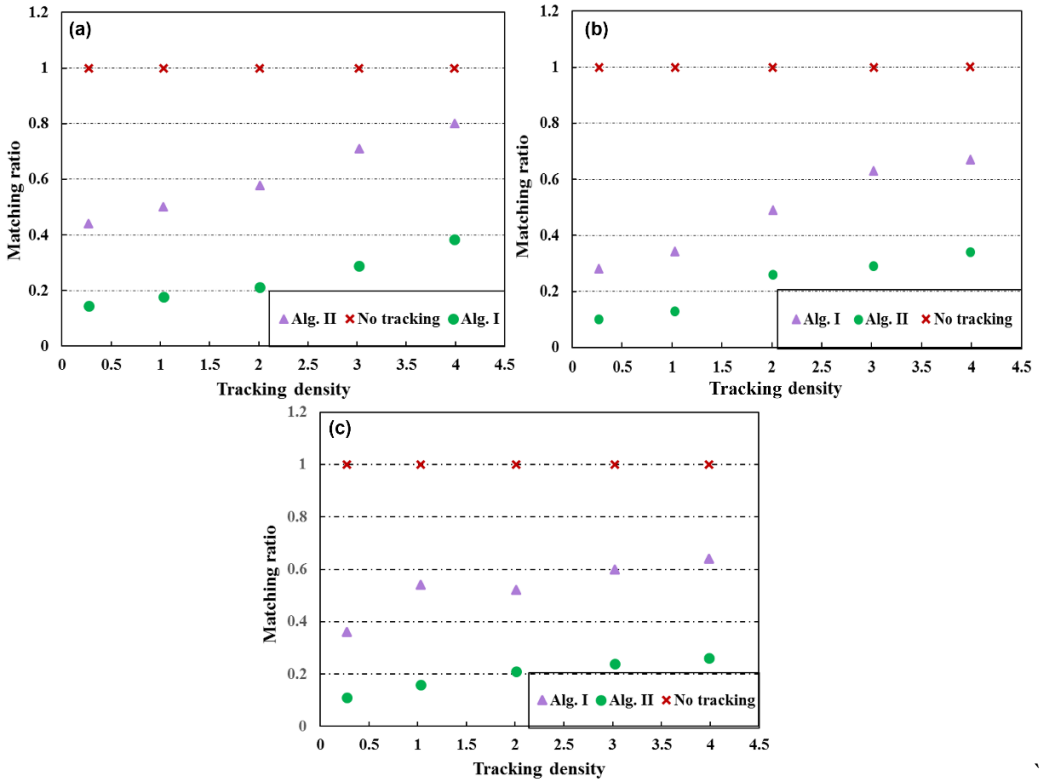


Fig. 3. Matching ratio vs. tracking density for (a) Linear flow, (b) Kovasznay flow and (c) Beltrami flow.

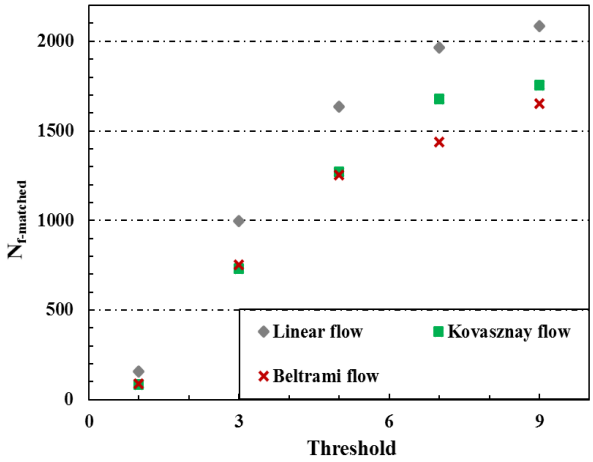


Fig. 4. Number of frames matched between the two systems vs. threshold

## 4 CONCLUSIONS

In this article, a method is presented to extend the measurement of the trajectory of particles in large ventilated cavities. The method makes use of several 3D PTV systems, each with multiple cameras, positioned next to each other to cover the entire measuring volume. In particular, a procedure is described for calibrating the 3D PTV systems involved, in order to express the particle trajectories in a common 3D coordinate system. Three types of flow based on the analytic solution of incompressible Navier–Stokes equations as well as a linear flow were generated. A method of linking trajectories, based on a similarity criterion is then detailed. The numerical results revealed that the performance of the proposed method is highly influenced by the accuracy of the tracking algorithm used by each 3D PTV system. As the particle tracking density increases, the performance of the multi 3D PTV algorithm increases. The numerical analysis presented in this paper reveals that the proposed method is capable of being utilized for airflow measurements in large inhabited areas. The proposed method will be experimentally evaluated as a future study.

## ACKNOWLEDGMENTS

The authors acknowledge funding from the *Conseil départemental de l'Allier* as well as the Université Clermont Auvergne postdoctoral grant 2020-2021.

## NOMENCLATURE

$m$ = *system*
$n$ = *system*
$XX$ = *3D reference frame*
$XX_c$ = *common 3D reference frame*
$R$ = *extrinsic parameters of camera*
$T$ = *extrinsic parameters of camera*
$u$ = *velocity in x direction*
$v$ = *velocity in y direction*
$x$ = *x-coordinate*
$y$ = *y-coordinate*

### Subscripts and superscript

$i$ = *number of camera*
$c$ = *common*

## REFERENCES

Adrian RJ (1991) Particle-imaging techniques for experimental fluid mechanics. Annual Review of Fluid Mechanics 261–304

Barker D (2012) Development of a scalable real-time Lagrangian particle tracking system for volumetric flow field characterization. University of Illinois at Urbana-Champagne

Biwole PH (2009) Large Scale Particle Tracking Velocimetry for Three-Dimensional Indoor Airflow Study. Institut National des Sciences Appliquees-Lyon

Ethier CR, Steinman DA (1994) Exact fully 3D Navier–Stokes solutions for benchmarking. International Journal for Numerical Methods in Fluids 19:369–375

Heikkila J, Silven O (1997) A Four-step Camera Calibration Procedure with Implicit Image Correction. In: In Proceedings of IEEE computer society conference on computer vision and pattern recognition. IEEE, pp 1106–1112

O'Sullivan J, Ferrua M, Love R, et al (2014) Airflow measurement techniques for the improvement of forced-air cooling, refrigeration and drying operations. Journal of Food Engineering 143:90–101

Popiolek Z, Melikov AK, Jorgensen FE, et al (1998) Impact of natural convection on the accuracy of low-velocity measurements by thermal anemometers with omnidirectional sensor. 1507

Resagk C, Lobutova E, Rank R, et al (2006) Measurement of large-scale flow structures in air using a novel 3D particle tracking velocimetry technique. 26–29

Wei Y (2010) Development of hybrid particle tracking algorithms and their applications in airflow measurement within an aircraft cabin mock-up

Zhang Z (1999) Flexible camera calibration by viewing a plane from unknown orientations. In: Proceedings of the Seventh IEEE International Conference on Computer Vision. pp 666–673